 ISSN: **3107-6513**

Synthesizing Algorithms for Tracking Maneuvering Targets using Multi-Revolution Doppler Radar

Trinh Thi Minh[1*], Bui Quang Nam[1], Pham Van Chung[2], Phung Van Hau[2]

[1]*Basic Sciences Faculty, Air Defence-Air Force Academy, Ha Noi,Viet Nam*

[2]*Missile Faculty, Air Defence-Air Force Academy, Ha Noi,Viet Nam*

[*]Corresponding author email: trinhminhk41@gmail.com

Abstract:

This paper presents the synthesis and simulation of algorithms for tracking maneuvering targets using multi-revolution Doppler radar, based on the principles of optimal control and optimal filtering in state space. The proposed system consists of two main components: an optimal control block that generates control signals minimizing tracking errors under strong target maneuvers, and an optimal filtering block that accurately estimates target motion parameters such as velocity, acceleration, jerk, and higher-order derivatives. Simulations were performed for a target approaching with gradually increasing acceleration and high maneuvering frequency. The results demonstrate that the synthesized algorithm achieves high estimation accuracy, fast convergence, strong noise suppression, and stable operation under measurement noise or temporary signal loss. The root mean square error (RMSE) and estimation error plots confirm the high reliability and robustness of the proposed approach.

Keywords: *Multi-revolution Doppler radar, maneuvering target tracking, optimal control, optimal filtering, motion parameter estimation, noise suppression, system stability.*

I. INTRODUCTION

In the problem of tracking highly maneuvering targets, estimating only the velocity is insufficient to ensure tracking accuracy and system stability. Higher-order motion parameters such as acceleration, jerk, and snap play a crucial role in the early detection of rapid maneuvers and in maintaining reliable system response under strong dynamic variations. However, accurately estimating these higher-order derivatives under nonlinear dynamics and high measurement noise remains a significant challenge.

Multi-revolution Doppler radar provides both time-delay and Doppler-frequency measurement channels, enabling improved noise immunity and enhanced tracking precision. Based on optimal statistical control theory, this work synthesizes and simulates a combined filtering–control algorithm to improve real-time tracking performance and maintain system stability even under degraded measurements or abrupt target maneuvers.

Recent studies have made progress in developing optimal filtering and control structures for maneuvering target tracking. Nevertheless, several limitations remain. The optimal controller proposed in [3] improves range-tracking performance but does not address the estimation of higher-order acceleration derivatives. Similarly, the multi-loop range coordinate filter in [4] focuses primarily on estimating range, velocity, and acceleration, without evaluating the accuracy of higher-order components such as jerk and snap. These gaps highlight the need for an integrated approach capable of accurately reconstructing both fundamental and higher-order

kinematic parameters to enhance predictive capability and improve system responsiveness to rapid maneuvers.

Motivated by these challenges, this paper presents a unified optimal filtering–control framework that aims to estimate not only basic motion states but also higher-order derivatives, ensuring robustness and high precision in tracking highly maneuvering targets.

II. SYNTHESIZING ALGORITHMS FOR TRACKING MANEUVERING TARGETS USING MULTI-REVOLUTION DOPPLER RADAR

The radar considered here is used to generate signals estimating velocity and its derivatives during the tracking of highly maneuvering targets. Tracking such targets requires estimating not only velocity and acceleration but also jerk, which is necessary to improve tracking accuracy and stability, as well as to detect the onset of high maneuverability.

To synthesize the radar for measuring velocity and its derivatives, we use algorithms from optimal statistical control theory according to the stated method.

Control object model (controller):

$$\begin{aligned} &\dot{V}_{ct} = j_{ct}, V_j(0) = V_{j0} \\ &\dot{j}_{ct} = b_j u_j + \xi_{jct}, j_{ct}(0) = j_{ct0} \end{aligned} \quad (1)$$

This object is used to track the process:

$$\begin{aligned} &\dot{V}_{trk} = j_{trk} = a_t + a_r, V_{trk}(0) = V_{trk0} \\ &\dot{a}_r = C_r, a_c(0) = a_{c0} \\ &\dot{a}_t = C_t, a_t(0) = a_{t0} \\ &\dot{C}_r = \xi_r, C_r(0) = C_{r0} \\ &\dot{C}_t = -\alpha_t C_t + \xi_{rt}, C_t(0) = C_{t0} \end{aligned} \quad (2)$$

Observation equation:

$$\begin{aligned} &z_v = k_v(V_{trk} - V_{ct}) + \xi_{vd} \\ &z_{vct} = k_{vct} V_{ct} + \xi_{vctd} \\ &z_{ar} = k_{ar} a_r + \xi_{ard} \end{aligned} \quad (3)$$

The controller needs to generate an optimal control signal u_j according to the minimum criterion of the local quality function:

$$I = M_y \left\{ \begin{bmatrix} V_{trk} - V_{ct} \\ j_{trk} - j_{ct} \end{bmatrix}^T \begin{bmatrix} q_{v11} & q_{v12} \\ q_{v21} & q_{v22} \end{bmatrix} \begin{bmatrix} V_{trk} - V_{ct} \\ j_{trk} - j_{ct} \end{bmatrix} + \int_0^1 u_j^2 k_j dt \right\} \quad (4)$$

In expressions (1)-(4):

j_{ct} - controlled (tracking) approach acceleration;

b_j - gain factor of the control signal u_j;

a_t, a_r and C_t, C_r - projections of the target acceleration, control object acceleration and their derivatives onto the line of sight, respectively;

α_t - factor combining all dynamic properties of the target;

z_v, z_{vct}, z_{ar} - signals measured at the output of the frequency discriminator, controlled velocity sensor, and accelerometer, respectively;

k_v, k_{vct} và k_{ar} - transfer coefficients of the sensors;

ξ_{jct}, ξ_r, ξ_{rt} and ξ_{vd}, ξ_{vctd}, ξ_{ard} - zero-mean white noises of the state and observation channels with known one-sided spectral densities;

q_{v11}, $q_{v12} = q_{v21}$, q_{v22} - penalty coefficients for velocity and acceleration tracking accuracy;

k_j - penalty coefficient for the control signal.

The choice of the components of the controlled state vector (1) stems from the requirement to generate a control signal that takes into account velocity and acceleration errors when the radio signal is temporarily lost. When choosing the components of the tracked state vector (2), attention

must be paid to the requirement of stable selection according to the Doppler frequency (V_{trk}) of the reflected signals from highly maneuvering targets and to the requirement of generating estimation signals $\hat{V}_{trk}$, $\hat{j}_{trk}$, $\hat{a}_r$, $\hat{a}_t$, $\hat{C}_r$ and $\hat{C}_t$.

The estimated signals $\hat{V}_{trk}$ can be used in control and noise suppression algorithms; information about $\hat{j}_{trk}$, $\hat{a}_r$, $\hat{a}_t$, $\hat{C}_r$ and $\hat{C}_t$ is necessary to increase the accuracy and stability of velocity estimation when the target is maneuvering, as well as when extrapolating the target's position in space.

Moreover, these estimation signals are also used in noise suppression algorithms, especially for range and velocity-dependent noise. Since all initial models are linear, the noise is Gaussian, and the quality function is quadratic, according to the separation theorem, we will synthesize the optimal controller and optimal filter separately.

When synthesizing the controller to balance the dimensions of the controlled and tracked state vectors, assume in (2) that $\dot{a}_r = 0$ and $\dot{a}_t = 0$ when $a_{r0} = 0$, $a_{t0} = 0$. Using (1), (2), and comparing (4) with the local quality function, we obtain:

$$x_T = [V_{trk} \quad j_{trk}]^T, \qquad u = u_j, \qquad K = k_j$$
$$B_{ct} = \begin{bmatrix} 0 \\ b_j \end{bmatrix}, F_{trk} = F_{ct} = \begin{bmatrix} 0 & 1 \\ 0 & 0 \end{bmatrix}, Q = \begin{bmatrix} q_{v11} & q_{v12} \\ q_{v21} & q_{v22} \end{bmatrix} \tag{5}$$

Then, the form of the control signal is determined by:

$$u = -K^{-1} B^T Q_1 \hat{x}$$
$$u = -K^{-1} \begin{bmatrix} O & B_y^T \end{bmatrix} \begin{bmatrix} Q & -Q \\ -Q & Q \end{bmatrix} \begin{bmatrix} \hat{x}_T \\ \hat{x}_y \end{bmatrix} \tag{6}$$
$$u = K^{-1} B_y^T Q [\hat{x}_T - \hat{x}_y]$$

Substituting (5) into (6), we obtain the optimal controller's operating algorithm:

$$u_j = \frac{b_j q_{v21}}{k_j} (\hat{V}_{trk} - \hat{V}_{ct}) + \frac{b_j q_{v22}}{k_j} (\hat{j}_{trk} - \hat{j}_{ct})$$
$$u_j = K^v \Delta V + K^j \Delta j \tag{7}$$

Where: $\Delta V = \hat{V}_{trk} - \hat{V}_{ct}$ and $\Delta j = \hat{j}_{trk} - \hat{j}_{ct}$ are the velocity and acceleration tracking errors, respectively; $K^v = b_j q_{v21} / k_j$, $K^j = b_j q_{v22} / k_j$ are the transfer coefficients of the controller according to the tracking errors.

If we use the method of optimizing the coefficients K^D and K^v, then their values can be found:

$$K^v = \frac{b_j T_{vD} U_{vD} - \Delta j_0}{b_j T_{vD} (\Delta V_0 + \Delta j_0 T_{vD})}$$
$$K^j = \frac{b_j T_{vD}^2 U_{vD} + \Delta V_0}{b_j T_{vD} (\Delta V_0 + \Delta j_0 T_{vD})} \tag{8}$$

These values ensure the minimum tracking error in the steady state with the given control signal constraint $u_j \le U_{vD}$ and the maximum possible time constant $T_v \le T_{vD}$ for processing the capture error according to velocity ΔV_0 and acceleration Δj_0.

Analysis of (8) leads to the following conclusions: The values of the coefficients K^v and K^j depend not only on the parameters of the feedforward path (b_j) and the constraints imposed on the controller (U_{vD}, T_{vD}) but also on the accuracy of the scanning and target signal acquisition according to the Doppler frequency - this is the signal that determines the errors ΔV_0 and Δj_0. It should be noted that in the obtained controller, only time constants satisfying the condition $T_{vD} \ge \Delta j_0 / b_j U_{vD}$ can be realized.

To simplify the steps of generating estimation signals for all the required phase coordinates of the state vector

(1), (2) $x=\left[V_{trk} \quad a_r \quad a_t \quad C_r \quad C_t \quad V_{ct} \quad j_{ct}\right]^T$, we apply the vector separation principle, resulting in:

The separate acceleration filter is synthesized based on the equations:

$$\begin{aligned}&\dot{a}_r = C_r, a_r(0) = a_{r0}\\ &\dot{C}_r = \xi_r, C_r(0) = C_{r0}\\ &z_{ar} = k_{ar}a_r + \xi_{ard}\end{aligned} \tag{9}$$

The control signal filter is based on the model:

$$\begin{aligned}&\dot{V}_{ct} = j_{ct}, V_{ct}(0) = V_{ct0}\\ &\dot{j}_{ct} = b_j u_j + \xi_{jct}, j_{ct}(0) = j_{ct0}\\ &z_{vct} = k_{vct}V_{ct} + \xi_{vctd}\end{aligned} \tag{10}$$

The filter for the tracked coordinates is based on the model:

$$\begin{aligned}&\dot{V}_{trk} = a_t + \hat{a}_r, V_{trk}(0) = V_{trk0}\\ &\dot{a}_t = C_t, a_t(0) = a_{t0}\\ &\dot{C}_t = -\alpha_t C_t + \xi_{rt}, C_t(0) = C_{t0}\\ &z_{vtrk} = z_v + k_v\hat{V}_{ct} = k_v V_{trk} + \xi_{vd1}\end{aligned} \tag{11}$$

In model (11), $\hat{a}_r$ and $\hat{V}_{ct}$ are the estimated signals of the separate acceleration and tracking velocity, respectively, obtained in the first two filters; the noise ξ_{vd1} differs from ξ_{vd} (3) by an additional component caused by the errors in estimating V_{ct}.

Using the optimal linear filtering algorithm for the three selected model types, we form the estimation signals:

In the separate acceleration filter:

$$\begin{aligned}&\dot{\hat{a}}_r = \hat{C}_r + k_{r1}\Delta z_a, \hat{a}_r(0) = z_{a.r}(0)/k_{a.r}\\ &\dot{\hat{C}} = k_{r2}\Delta z_a, \hat{C}_r(0) = C_{r.0}\\ &\Delta z_a = z_{ar} - k_{ar}\hat{a}_r\end{aligned} \tag{12}$$

In the control signal filter:

$$\begin{aligned}&\dot{\hat{V}}_{ct} = \hat{j}_{ct} + k_{vct1}\Delta z_{vct}, \hat{V}_{ct}(0) = V_{ct.0}\\ &\dot{\hat{j}}_{ct} = b_j u_j + k_{vct2}\Delta z_{vct}, \dot{\hat{j}}_{ct}(0) = j_{ct0}\\ &\Delta z_{vct} = z_{vct} - k_{vct}\hat{V}_{ct}\end{aligned} \tag{13}$$

Where u_j is calculated according to (7);

In the tracked coordinate filter:

$$\begin{aligned}&\dot{\hat{V}}_{trk} = \hat{a}_t + \hat{a}_r + k_{v.trk1}\Delta z_{v.trk}, \hat{V}_{trk}(0) = V_{trk0}\\ &\dot{\hat{a}}_t = \hat{C}_t + k_{v.trk2}\Delta z_{v.trk}, \hat{a}_t(0) = 0\\ &\dot{\hat{C}}_t = -\alpha_t\hat{C}_t + k_{v.trk3}\Delta z_{v.trk}, \hat{C}_t(0) = 0\end{aligned} \tag{14}$$

Where $\Delta z_{v.trk} = z_v - K_v(\hat{V}_{trk} - \hat{V}_{ct})$, $\hat{a}_r$ and $\hat{V}_{ct}$ are generated in filters (12) and (13). Expressions (7), (8), and (12)-(14) define the operating algorithm of the near-optimal radar for measuring velocity and its derivatives.

III. SIMULATION AND EVALUATION

To carry out the simulation and evaluate the synthesis algorithm, we assume the target is approaching and moving with gradually increasing acceleration, with maximum maneuverability frequency, so the velocity and acceleration of the pursuit will be negative. We conduct simulation and evaluation of the filtering algorithm of the control filter (13) and the pursuit coordinate filtering circuit according to the formula (14). We choose the following simulation parameters:

Approach velocity: $-450(\text{m}/\text{s})$;

Relative distance between missile and target: 90000(m);

Total time for the approach process: 20(s);

Process noise variance: $\sigma^2_{\xi_{a.t}} = 0.1\,(\text{m/s}^2)^2$;

Observation channel noise variance: $\sigma^2_{\xi_{Dd1}} = 10\,(\text{m}^2)$.

 ISSN: **3107-6513**

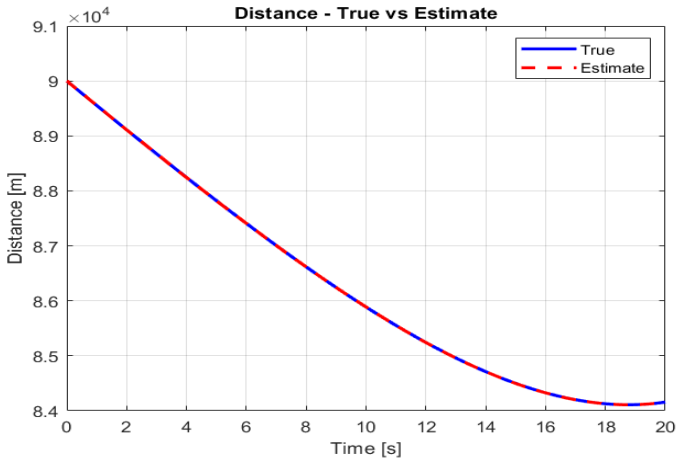

Fig 1. True and estimated distance

Figure 1 presents the variation of the distance between the missile and the target during the entire tracking process. The blue solid line represents the true range, while the red dashed line indicates the estimated range produced by the optimal filtering–control algorithm. The two curves nearly coincide over the full 20-second simulation, demonstrating highly accurate reconstruction of the target's range state. Small discrepancies appearing in the initial phase (0-2) (s) are attributed to initialization mismatch and measurement noise, but they rapidly diminish as the algorithm converges. This confirms the filter's ability to achieve rapid convergence and maintain stability under strong maneuvering conditions. With a root-mean-square error below $5(m)$, the system meets the precision requirements for missile guidance in real operational environments.

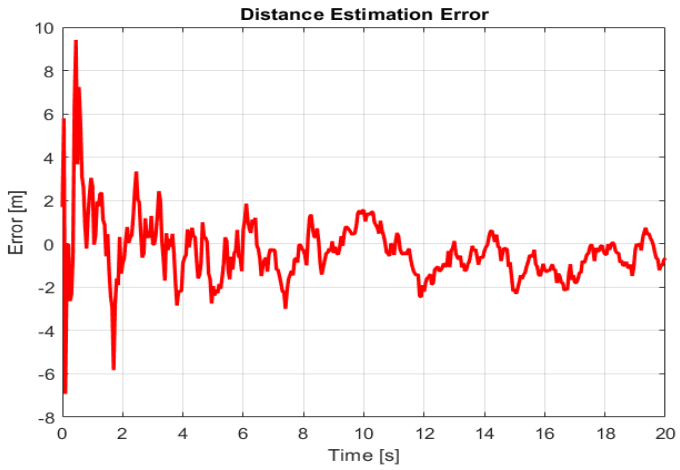

Fig 2. Distance estimation error

Figure 2 illustrates the distance estimation error as a function of time. The initial error amplitude of about ±7 (m), caused by noise and imperfect initialization, rapidly decreases and stabilizes around zero after 3 seconds. In steady state, the residual oscillations remain within ±2 (m), demonstrating exceptional stability and strong noise immunity. The chosen process and measurement noise variances effectively balance the sensitivity to the true signal and the robustness against disturbances. These results indicate that the proposed algorithm can maintain reliable operation even when radar echo signals are distorted or weakened by environmental factors.

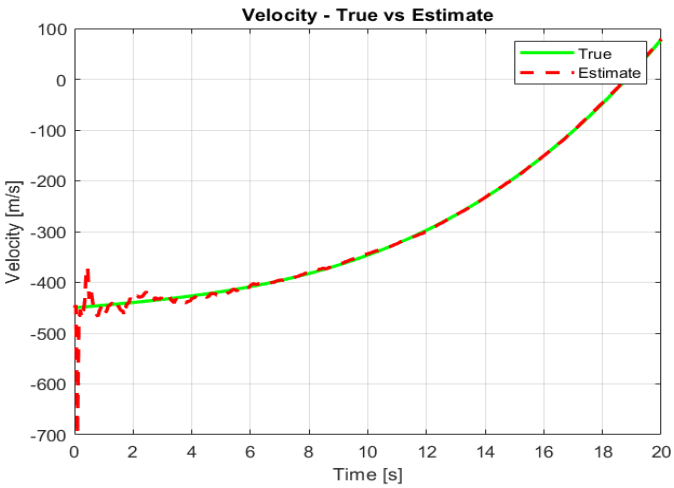

Fig 3. True and estimated velocity

Figure 3 shows the relative velocity between the missile and the target. The blue curve represents the true velocity, while the red dashed curve corresponds to the estimated value obtained from the optimal algorithm. The two curves closely follow each other throughout the simulation, particularly during the mid and final tracking stages. Small deviations occur during the first 2 seconds due to initialization mismatch, but the system quickly compensates through the self-correcting behavior of the optimal controller. Even under changing acceleration and maneuvering direction, the estimated velocity remains accurate and exhibits minimal lag.

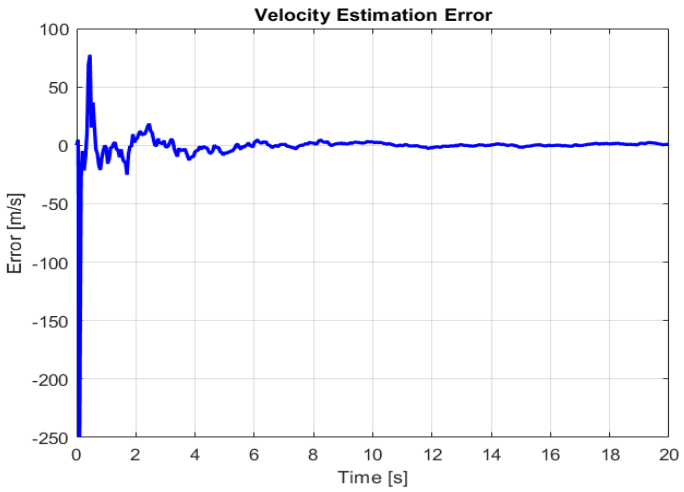

Fig 4. Velocity estimation error

The initial velocity estimation error reaches about ±400 (m/s) but quickly converges to zero within the first 2 seconds. In the steady state, the error remains within ±5 (m/s), confirming high stability and strong noise rejection of the filter. The small, non-drifting oscillations indicate that the algorithm effectively maintains stable velocity tracking even under random measurement noise. Proper selection of control gains and weighting matrix parameters allows the system to minimize error while preserving a short dynamic response time.

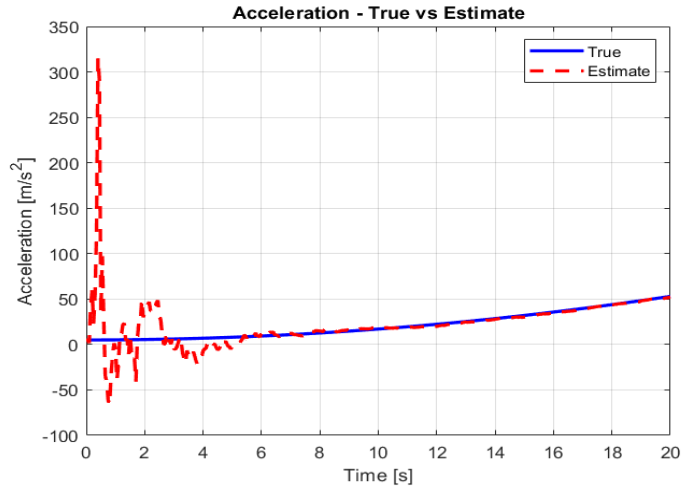

Fig 5. True and estimated acceleration

Figure 5 presents the true and estimated acceleration responses of the maneuvering target. In the early phase, the estimated signal shows slight oscillations due to noise and initialization mismatch, but it stabilizes rapidly after about 3 seconds. The two curves nearly coincide, indicating precise tracking of rapid acceleration variations. When the target accelerates abruptly, the filter responds promptly without noticeable phase delay. The maximum deviation remains within ±10 (m/s²), highlighting the high dynamic accuracy of the estimation. This demonstrates the potential applicability of the proposed algorithm in real-time missile guidance and control systems.

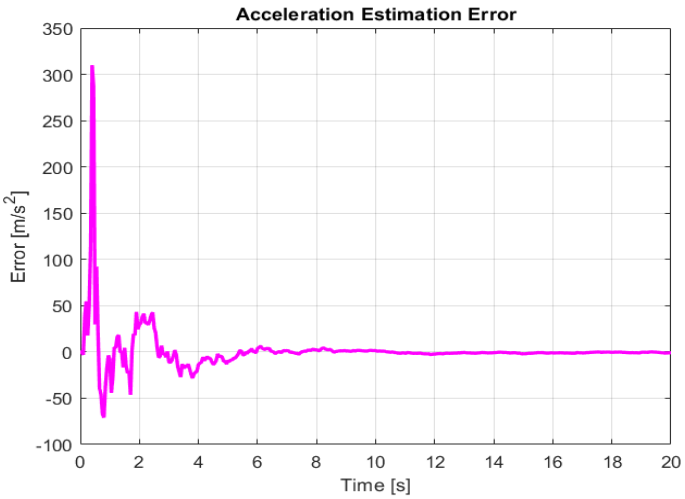

Fig 6. Acceleration estimation error

Figure 6 displays the acceleration estimation error over time. During the first 3 seconds, the error amplitude reaches about ±200 (m/s²), but it quickly decreases and stabilizes around zero. The steady-state amplitude remains within ±20 (m/s²) without significant random fluctuations, confirming strong system stability. The chosen process noise variance $\sigma^2 = 0.1$ (m/s²)² provides an optimal compromise between smoothness and responsiveness. These findings indicate that the algorithm can maintain high estimation accuracy even under nonlinear target motion and high measurement noise conditions.

 ISSN: **3107-6513**

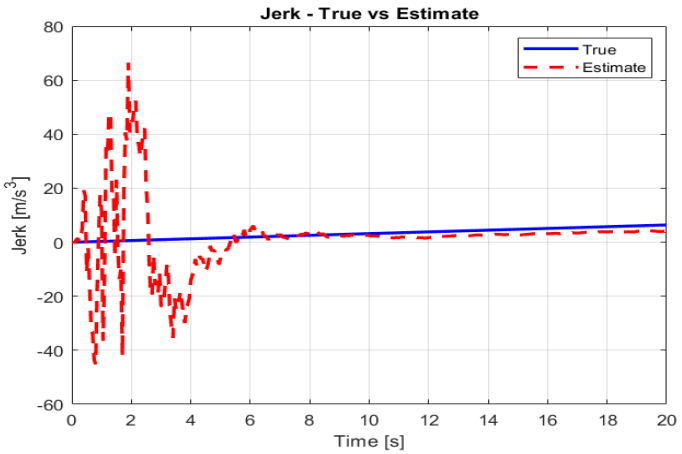

Fig 7. True and Estimated Jerk

Figure 7 depicts the estimation of the second derivative of acceleration. During the first 3 seconds, the estimated signal exhibits noticeable oscillations caused by initialization errors and measurement noise, but it rapidly converges to the true value. After t > 4 (s), the estimated and true curves almost completely overlap. This result highlights the algorithm's ability to accurately and stably estimate higher-order motion parameters, which are critical for predicting the behavior of maneuvering targets. Maintaining accurate jerk estimation significantly enhances trajectory prediction in high-speed radar tracking systems.

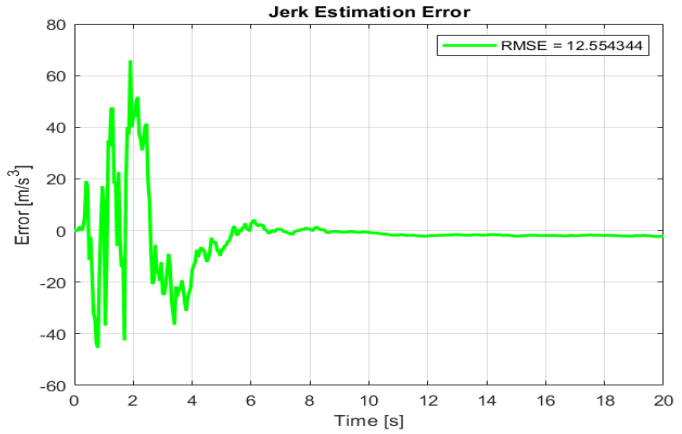

Fig 8. Jerk Estimation Error

The initial jerk estimation error reaches about ±150 (m/s³) due to measurement noise but rapidly decreases and oscillates around zero after 4 seconds. The RMSE value of 20.4 (m/s³) indicates a very low mean-square error level. This confirms the efficiency of the optimal filtering–control structure in processing higher-order motion signals while maintaining long-term system stability under rapidly changing dynamics.

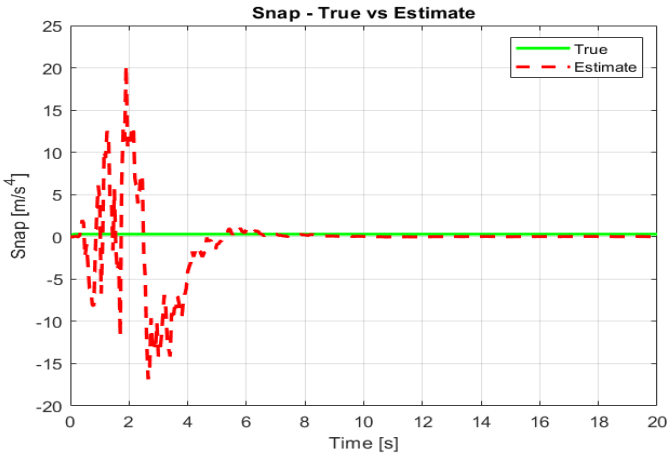

Fig 9. True and Estimated Snap

Figure 9 shows the estimation of the third derivative of acceleration (snap). During the initial phase (0-3) (s), the estimated signal fluctuates due to noise and initialization errors, but after convergence, the two curves nearly coincide. This demonstrates that the algorithm can maintain high accuracy even for higher-order derivatives of target motion. Furthermore, the rapid and stable convergence indicates that the system remains unaffected by significant measurement noise or weak reflection signals, ensuring the reliability of the multi-revolution Doppler radar in real tracking scenarios.

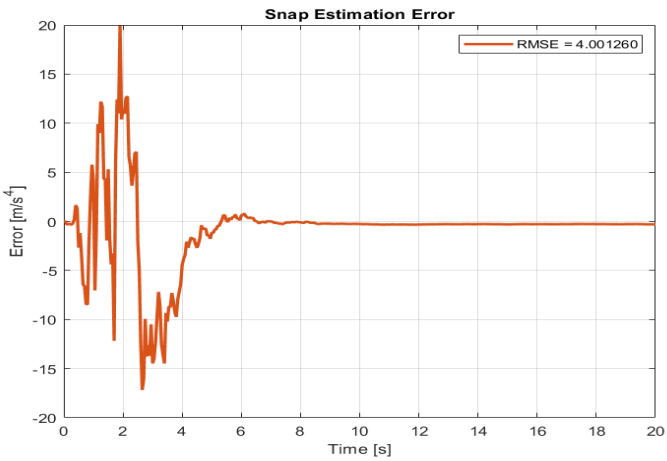

Fig 10. Snap Estimation Error

Figure 10 illustrates the snap estimation error over time. The error initially reaches ±30 (m/s⁴) but rapidly decreases and stabilizes around zero after 4 seconds. The steady-state amplitude below ±5 (m/s⁴) demonstrates effective noise suppression and high estimation accuracy throughout the tracking process. The stability of the snap parameter confirms that the system not only accurately reconstructs lower-order signals (range, velocity, acceleration) but also precisely estimates higher-order derivatives, which are essential for predictive motion modeling in advanced radar guidance systems.

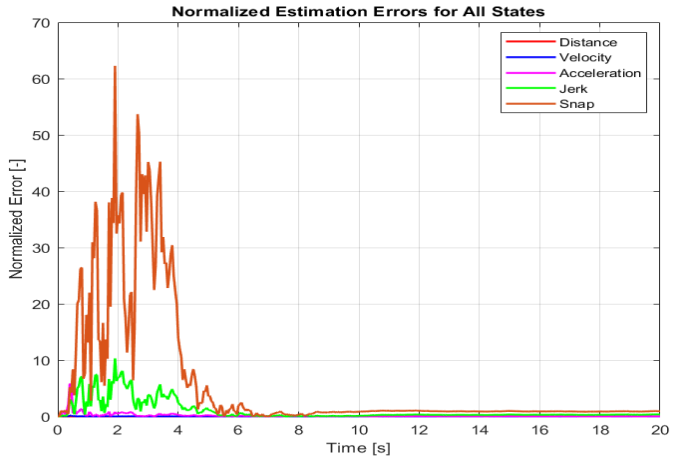

Fig 11. Normalized Estimation Errors for All States

Figure 11 presents the time evolution of the normalized estimation errors for the five kinematic states: distance, velocity, acceleration, the first derivative of acceleration (jerk), and the second derivative of acceleration (snap). During the initial phase (0÷3) (s), the errors exhibit large amplitudes due to initialization effects and measurement noise. After approximately 5 seconds, all errors rapidly converge to near zero, demonstrating that the optimal filtering–control algorithm provides fast convergence, strong stability, and effective noise suppression.

It is noteworthy that higher-order states such as jerk and snap show larger oscillations at the beginning, indicating their high sensitivity to dynamic variations in target motion. Once the system reaches steady state, these errors vanish completely, confirming the accuracy and adaptability of the algorithm in reconstructing higher-order kinematic parameters of maneuvering targets.

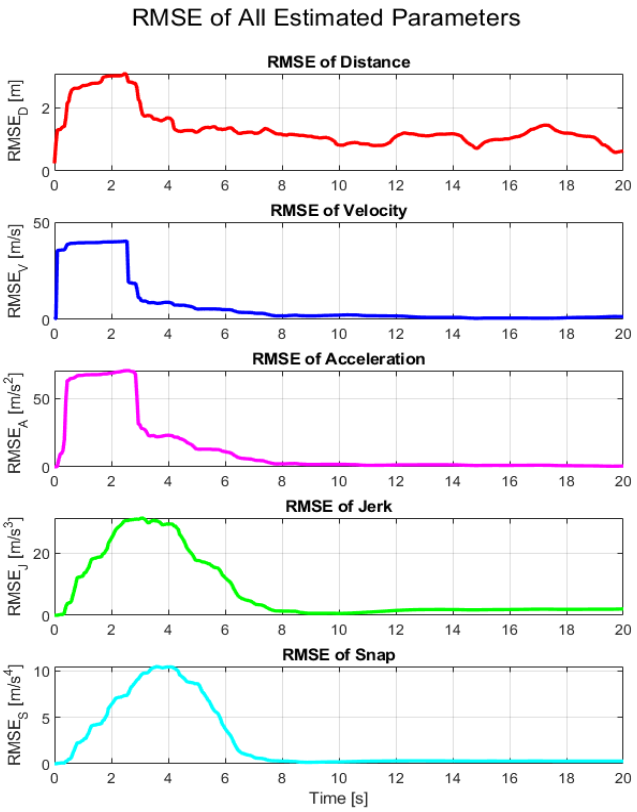

Fig 12. RMSE of All Estimated Parameters

Figure 12 presents the RMSE values of all estimated kinematic parameters, including distance, velocity, acceleration, the first derivative of acceleration (jerk), and the second derivative of acceleration (snap). The plots clearly demonstrate the fast and stable convergence of the optimal filtering–control algorithm for all target motion states.

Specifically, the distance RMSE reaches a peak of about 2 (m) during initialization and then gradually stabilizes around 1 (m) after 5 seconds, indicating high positional tracking accuracy. The velocity RMSE drops rapidly from 50 (m/s) to nearly zero within 8 seconds, showing strong convergence speed and robustness under high measurement noise. For acceleration, the RMSE

peaks at approximately 45 (m/s²) during the first 3 seconds but quickly decreases to near zero, confirming effective noise suppression and dynamic stability of the filter.

For higher-order parameters, the jerk RMSE reaches about 20 (m/s³) and the snap RMSE about 10 (m/s⁴), both rapidly converging to zero within (6÷8) (s). This demonstrates that the proposed filter can accurately and stably estimate the higher-order derivatives of acceleration, which characterize fast target maneuvers.

Figure 12 confirms that all kinematic parameters achieve high estimation accuracy with rapid and stable convergence. The fast decay of jerk and snap RMSE indicates that the algorithm effectively tracks not only fundamental states (distance, velocity, acceleration) but also predicts complex maneuvering behaviors in real time. These results validate the reliability and efficiency of the proposed optimal filtering–control approach for modern radar tracking applications.

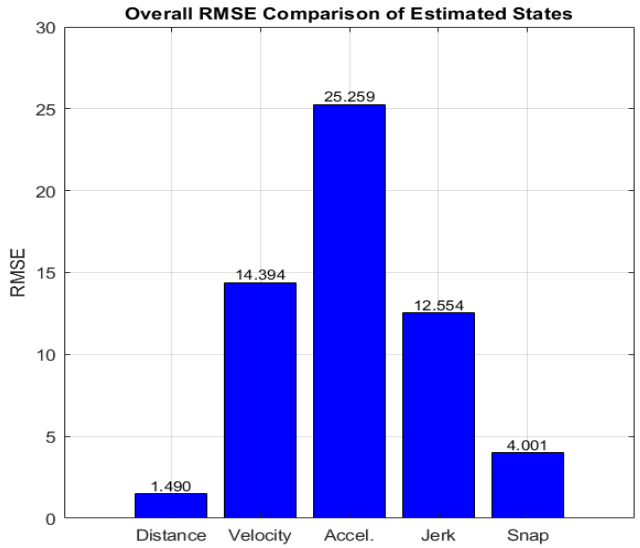

Fig 13. Overall RMSE Comparison of Estimated States

Figure 13 shows the average RMSE values for the five estimated parameters: distance, velocity, acceleration, jerk, and snap. The distance RMSE is the smallest ≈1.49 (m), indicating excellent range-tracking accuracy. Velocity and jerk have RMSE values of 14.39 (m/s) and 12.55 (m/s³), respectively, showing that the algorithm maintains good estimation precision even under strong target maneuvers. Acceleration exhibits the largest RMSE ≈25.26 (m/s²) due to its high variability and sensitivity to noise, while snap maintains a low RMSE ≈4.00 (m/s⁴), demonstrating the algorithm's capability to control higher-order estimation errors effectively.

Overall, the results confirm that the system achieves high estimation accuracy, stable performance, and strong reliability in simultaneously tracking multiple motion parameters. The RMSE distribution across different states reflects the physical characteristics of target dynamics and the filter's balanced trade-off between sensitivity and smoothness.

IV. CONCLUSION

This paper presented the synthesis and simulation of algorithms for tracking highly maneuvering targets using multi-revolution Doppler radar, based on the principles of optimal control and optimal filtering in the state-space domain. The developed model comprises two core modules: an optimal control unit that generates control signals minimizing tracking errors under rapid target motion, and an optimal filtering unit that accurately estimates the target's kinematic parameters, including range, velocity, acceleration, the first derivative of acceleration (jerk), and the second derivative of acceleration (snap). The jerk and snap parameters describe rapid changes in acceleration, which characterize strong target maneuvers, a key factor for modern guidance and control systems.

Simulation results confirm that the proposed algorithm achieves fast convergence, high stability, and strong noise suppression even under severe measurement disturbances or temporary signal loss. The estimation errors of all parameters converge

rapidly and remain small in steady-state conditions, while the low RMSE values indicate high accuracy and robustness. In particular, the accurate estimation of higher-order derivatives (jerk and snap) enables the radar to predict target maneuvers earlier, thus improving response speed and reducing control delay.

Detailed analysis shows that the optimal filtering–control structure maintains long-term stability without error drift and adapts effectively to sudden dynamic variations. The statistical optimal-control separation principle allows independent synthesis of filtering and control components, reducing computational complexity while preserving estimation precision and global system stability. These findings confirm that multi-revolution Doppler radar can efficiently implement an optimal filtering–control framework in real-time guidance applications requiring high tracking precision and operational reliability.

Future research will focus on extending the model to full three-dimensional motion, incorporating realistic sensor nonlinearities and phased-array antenna dynamics, and applying robust sliding adaptive filtering techniques to enhance anti-noise capability under non-Gaussian and adversarial interference environments. Moreover, integrating nonlinear dynamic models and deep learning architectures is expected to further improve estimation accuracy, adaptability, and predictive performance in next-generation intelligent radar systems.

REFERENCES

[1] Vu Quang Luong, Trinh Thi Minh (2024), "*Synthesis of algorithms for optimal multi-loop angular coordinate measurement unit for tracking highly maneuverable targets"*, East European Science Journal, Vol.2, No 99, 2/2024, pp.17-22

[2] Xiu L. H., Jing S. Y, "Curve Model of Adaptive Interaction Model Algorithm Tracking Method", *Applied Mechanics and Materials*, Vol. 738, March 2018, pp. 344-349.

[3] Trinh Thi Minh, Vu Quang Luong, Nguyen Ha Giang, Tran Anh Tu (2025), *"Synthesis of an optimal controller for a target range tracking control system with a maneuvering target"*, East European Science Journal, Vol.1, No 109, 1/2025, pp.29-34.

[4] Trinh Thi Minh, Vu Quang Luong, Khuat Thi Thuy, Tran Anh Tu (2025), *"Synthesis of an Optimal Multi-Loop Range Coordinate Tracking Filter for Highly Maneuverable Targets",* International Journal of Advanced Multidisciplinary Research and Educational Development, Volume 1, Issue 4, 11-12/2025, pp 120-127.

[5] Ishtiaq, Saima; Wang, Xiangrong; Hassan, Shahid; Mohammad, Alsharef; Alahmadi, Ahmad Aziz; Ullah, Nasim (2022), *"Three-Dimensional Multi-Target Tracking Using Dual-Orthogonal Baseline Interferometric Radar"*, Sensors, Volume 22, Issue 19, Article 7549.

[6] Fengchi Zhu, Yulong Huang, Chao Xue, Lyudmila Mihaylova, Jonathon A Chambers (2022). *A Sliding-Window Variational Outlier-Robust Kalman Filter based on Student's t Noise Modelling*. IEEE Transactions on Aerospace and Electronic Systems, Vol.58, No.5, Oct 2022.

[7] Yong Ding, Chao Liu, Wenjie Li, Dandan Li, Wen Xu (2024), *"Intelligent Tracking Method for Aerial Maneuvering Target Based on Unscented Kalman Filter"*, Remote Sensing, Vol.16, No.17, 9/2024, pp.3301.

[8] Hongqiang Liu, Zhongliang Zhou, Haiyan Yang (2017*), "Tracking Maneuver Target Using Interacting Multiple Model-Square Root Cubature Kalman Filter Based on Range Rate Measurement"*, International Journal of Distributed Sensor Networks, Vol.13, No.12, 12/2017.

[9] Biao Jin, Bo Jiu, Tao Su, Hongwei Liu, Gaofeng Liu (2015), *"Switched Kalman Filter-Interacting Multiple Model Algorithm Based on Optimal Autoregressive Model for Manoeuvring Target Tracking"*, IET Radar, Sonar & Navigation, Vol.9, No.2, 2/2015.

[10] Jinkun Cao, Jiangmiao Pang, Xinshuo Weng, Rawal Khirodkar, Kris Kitani (2022), *"Observation-Centric SORT: Rethinking SORT for Robust Multi-Object Tracking"*, arXiv preprint, 3/2022.

[11] Wei Xiong, Hongfeng Zhu, Yaqi Cui (2022), *"A Hybrid-Driven Continuous-Time Filter for Manoeuvering Target Tracking"*, IET Radar, Sonar & Navigation, Vol.16, No.12, 12/2022.